

Cell Reports, Volume 24

Supplemental Information

**Molecular Deconvolution Platform
to Establish Disease Mechanisms
by Surveying GPCR Signaling**

Ikuo Masuho, Sreenivas Chavali, Brian S. Muntean, Nickolas K. Skamangas, Kristina Simonyan, Dipak N. Patil, Grant M. Kramer, Laurie Ozelius, M. Madan Babu, and Kirill A. Martemyanov



Figure S2. Evaluation of the structural model of G α olf. Related to Figure 3.

Since G α olf shares 88% amino-acid identity with G α s, the homology model of G α olf was constructed on the basis of the crystal structure of the G α s (1AZT). The G α s crystal structure (green) and the G α olf model (gray) were overlaid. The G α olf model results in root mean square deviations of 0.31 Å, indicating a good fit between the model and the reported structure.

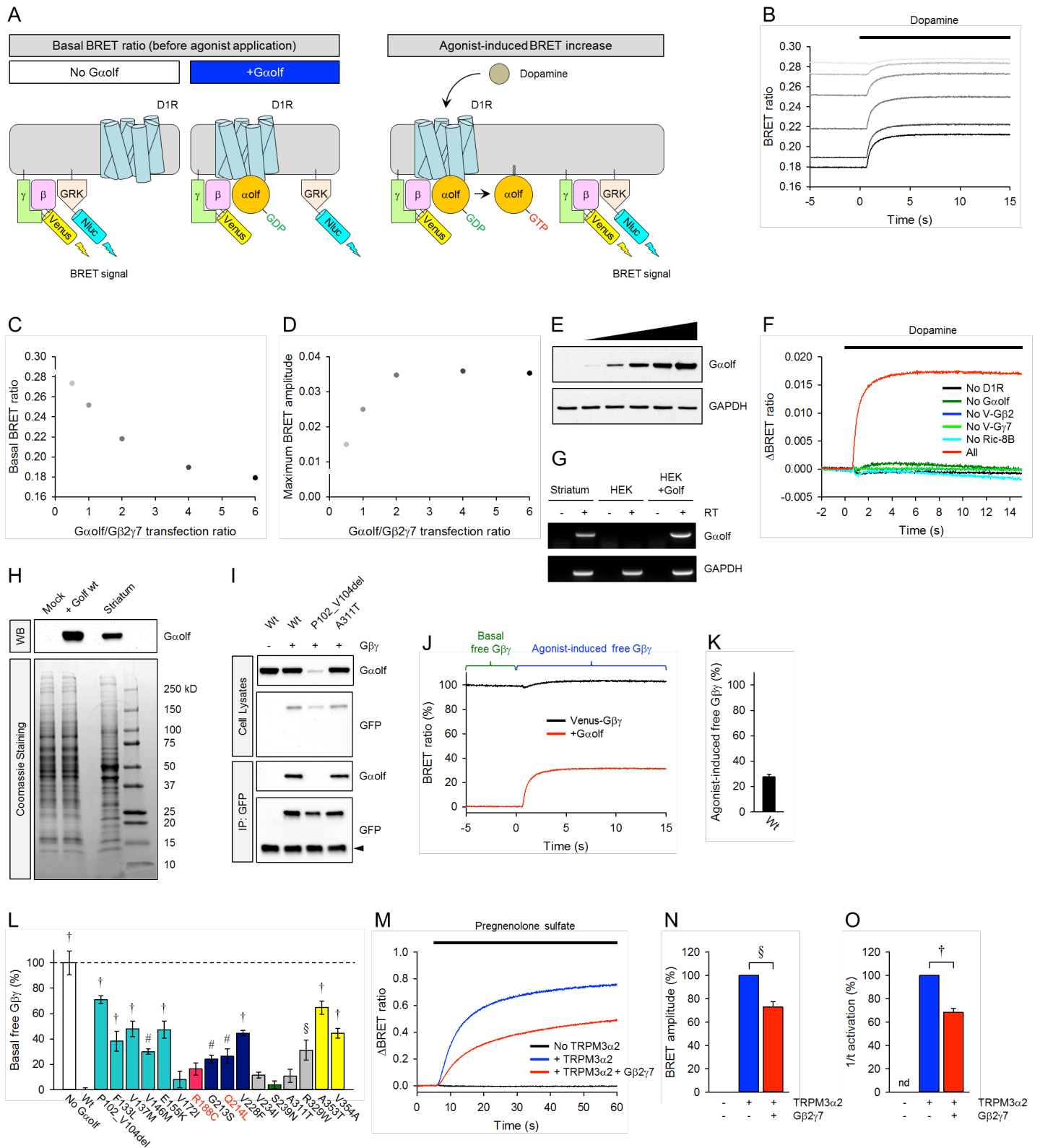


Figure S3. Reconstitution of D1R-G α olf/G β 2 γ 7 pathway in HEK293T/17 cells and effects of G α olf mutations on G β γ signaling. Related to Figure 4.

A, The assay design for optimizing stoichiometric G α olf/G β 2 γ 7 trimer. In the absence of exogenous G α subunit, expression of masGRK3ct-Nluc with Venus-G β 2 γ 7 produces masGRK3ct-Nluc-bound Venus-G β 2 γ 7, and

results in high basal BRET signal. In this condition, agonist application does not increase BRET signal because there is no functional trimer formation. Additional expression of G α olf sequesters Venus-G β 2 γ 7 from masGRK3ct-Nluc and decreases the BRET signal. Under optimal condition, agonist application induces robust BRET increase, indicating G α olf/G β 2 γ 7 trimer formation. Therefore, the transfection condition producing 1:1 ratio of G α olf and G β 2 γ 7 is expected to minimize basal BRET ratio (before agonist application) and maximize agonist-induced BRET response. **B-E**. Experimental optimization of the stoichiometry of G α olf and Venus-G β 2 γ 7. HEK293T/17 cells were transfected with plasmids encoding D1R, G α olf, Venus-G β 2 γ 7, masGRK3ct-Nluc. **B**, The stoichiometry of G α olf and Venus-G β 2 γ 7 were optimized by titrating the amount of G α subunits against a constant amount of Venus-G β 2 γ 7. Effect of increasing G α with constant Venus-G β 2 γ 7 for transient transfection on the basal BRET ratio and the agonist-induced maximum BRET amplitude were examined. 100 μ M dopamine was applied to the transfected cells. **C-D**, Basal BRET ratios and maximum BRET amplitudes are plotted as a function of the ratio of the amount of the G α subunit construct to the amount of the Venus-G β 2 γ 7 construct used for transfections, in the absence (basal BRET) (**C**) and presence (maximum amplitude) of a saturating concentration of dopamine (100 μ M) (**D**). Each data point represents the mean \pm SEM of twelve replicates. Graphs shown here are the representative data from two independent experiments with similar result. **E**, Western blot analysis was performed with anti-G α olf antibody. GAPDH was also probed with a specific antibody as a loading control. **F**, Verification of the reconstitution of D1R-G α olf/G β 2 γ 7 signaling. Each of the signaling molecule was removed from the optimized transfection condition and the BRET assay was performed with transfected cells. **G**, Semiquantitative analysis of G α olf mRNA in the striatum (*left*) and HEK293T/17 cells without (*middle*) or with transfection of Golf (*right*) were performed by RT-PCR. Reverse transcriptase was heat-inactivated under the minus (-) condition. The heat inactivation step was omitted under the plus (+) condition. RT-PCR with specific primers for GAPDH was performed as a control. **H**, Expression levels of G α olf protein in HEK293T/17 cells without (*left*) or with transfection of Golf (*middle*), and the striatum (*right*) were determined by Western blotting (*bottom*). Coomassie brilliant blue staining of a SDS-PAGE gel loaded with 10 μ g of cell or tissue lysate were performed as a loading control (*top*). **I**, Coimmunoprecipitation was performed with cells transfected with G α olf with or without Venus-G β 2 γ 7. Transfection conditions were indicated above. The bands indicated by an arrow head are antibody light chains, showing the same amount of anti-GFP antibody was used for immunoprecipitation. **J**, Percentage of agonist-induced free G β 2 γ 7 dimer. Basal BRET ratio under the presence of stoichiometric trimer formation was presented as 0% free G β 2 γ 7. Maximum free G β 2 γ 7 dimer was determined by transfection without G α olf. Percentage of agonist-induced free G β 2 γ 7 dimer was plotted as a bar graph (**K**). **L**, Percentage of free G β 2 γ 7 dimer produced by mutant G α olf subunits before agonist application was determined and plotted as a bar graph (n = 3 independent experiments).

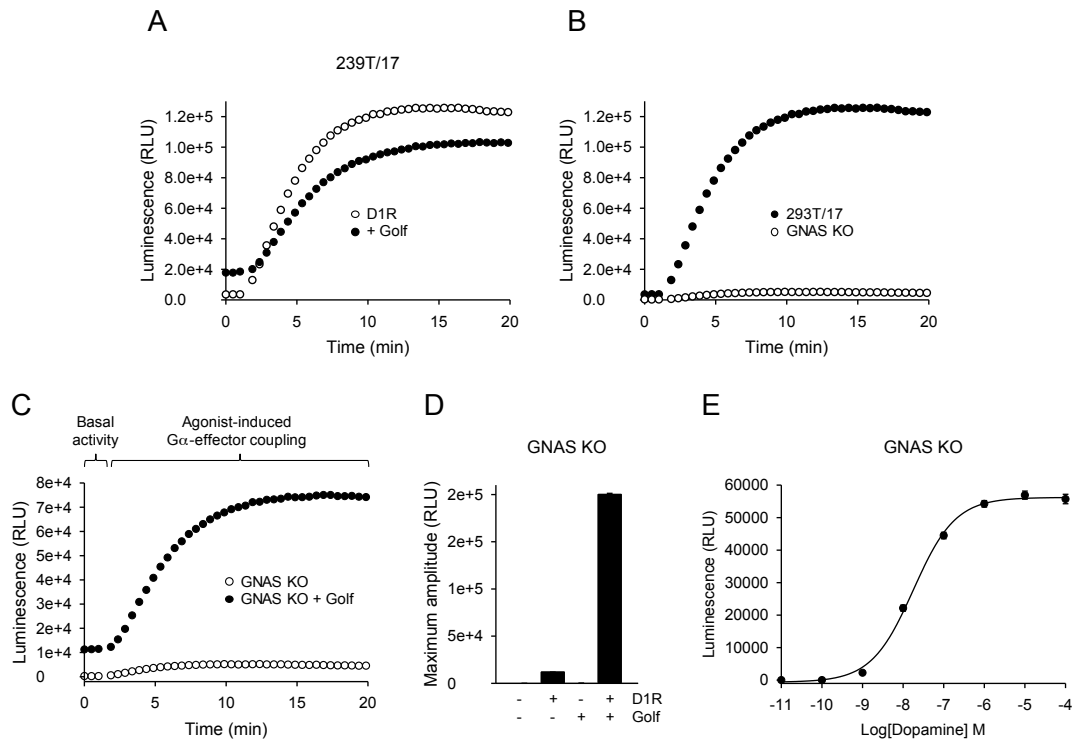


Figure S4. Generation of a GNAS knockout cell line and reconstitution of D1R-Golf-AC signaling in the cells. Related to Figure 5.

A, Agonist-induced cAMP production detected with GloSensor cAMP sensor. The agonist-induced cAMP production of HEK293T/17 cells transfected with (filled circle) or without (open circle) Gαolf. All cells were transfected with D1R and GloSensor-22F cAMP sensor. Values represent means \pm SEM from three independent experiments each performed with four replicates. **B**, Agonist-induced cAMP production of HEK293T/17 cells (filled circle) and *GNAS* KO cell line (open circle). All cells were transfected with D1R and GloSensor-22F cAMP sensor. Values represent means \pm SEM from three independent experiments each performed with four replicates. **C**, *GNAS* knockout cells were transfected with D1R and GloSensor-22F cAMP sensor together with (filled circle) or without (open circle) Gαolf. 100 μ M dopamine-induced cAMP production was recorded. **D**, Confirmation of selective D1R-Golf. D1R and Golf were transfected with GloSensor-22F cAMP sensor as indicated at the bottom of the bar graph. **E**, Determination of EC50. Dose-response relationship was examined using *GNAS* KO cells transfected with D1R, Gαolf, and GloSensor-22F cAMP sensor.

Table S1. Genotype and clinical phenotype features of dystonia mutations used in the study.

Related to Figure 2.

| Protein variant | Mutation site | Mutation type | Number of carrier reported | Ethnicity | Gender | Age of onset (years) | Dystonia distribution | Inheritance | Familial /sporadic | Reference |
|-----------------|-------------------|-------------------|----------------------------|------------------|-------------|---------------------------|---------------------------------|-------------|--------------------|-------------------------------|
| P102_V104del | α -helical | In frame deletion | 1 | Caucasian | M | 20 | Fo | Het | Familial | Fuchs et al., 2013 |
| F133L | α -helical | Missense | 1 | Brazilian | F | 23 | S | Het | Unknown | Dos Santos et al., 2016 |
| V137M | α -helical | Missense | 7 | Caucasian | 4xF and 3xM | 7, 19, 22, 26, 31, 44, 50 | 6xS, 1xG | Het | Familial | Fuchs et al., 2013 |
| V146M | α -helical | Missense | 3 | German | 1xF | 63 | 1xS | Het | Sporadic | Zech et al., 2014 |
| E155K | α -helical | Missense | 2 | Caucasian | 2xM | 17, 18 | 1xFo, 1xS | Het | Familial | Fuchs et al., 2013 |
| V172I | α -helical | Missense | 1 | Amish-Mennonites | F | 21 | S | Het | Sporadic | Saunders-Pullman et al., 2014 |
| G213S | Switch II | Missense | 1 | German | M | 40 | Fo (no hyposmia) | Het | Unknown | Kumar et al., 2014 |
| V228F | Switch II | Missense | 5 | African-American | 3xF, 2xM | 45, 50, 50, 63, N/A | 1xFo, 3xS, 1xG with 2xMicrosmia | Het | Familial | Vemula et al., 2013 |
| V234I | GTPase | Missense | 1 | Caucasian | M | 36 | Fo | Het | Sporadic | Putzel et al., 2016 |
| S239N | Switch III | Missense | 1 | N/A | N/A | N/A | N/A | Het | Unknown | This study |
| A311T | GTPase | Missense | 1 | German | N/A | N/A | N/A | Het | Sporadic | Kumar et al., 2014 |
| R329W | GTPase | Missense | 2 | Turkish | F | 11 and 15 | 2xG | Ho | Familial | Masaho et al., 2016 |
| A353T | TCAT motif | Missense | 1 | Japanese | F | 44 | Fo (no hyposmia) | Het | Unknown | Kumar et al., 2014 |
| V354A | TCAT motif | Missense | 1 | Serbian | F | 40 | Fo | Het | Sporadic | Dobričić et al., 2014 |

M = Male, F = Female

Fo = Focal, S = Segmental, G = Generalized

Het = Heterozygous, Ho = Homozygous

Table S2: Criteria for deleteriousness classification of amino acid substitutions using different methods. Related to Figure 2.

| Predictor | Classification criteria |
|---|---|
| Polyphen: Polyphen2 HDIV score (pp2_hdiv) | Deleterious: Probably damaging (pp2_hdiv \geq 0.957), P: possibly damaging; Tolerated: Benign (pp2_hdiv \leq 0.452) There were no DYT25 mutations in the possibly damaging category ($0.453 \leq$ pp2_hdiv \leq 0.956) (Wang et al., 2010) |
| SIFT | Deleterious: SIFT score \leq 0.05; Tolerated: SIFT score $>$ 0.05 (Wang et al., 2010) |
| CADD | Deleterious: CADD PHRED-scaled score $>$ 20; Tolerated: CADD PHRED-scaled score \leq 20 (Kircher et al., 2014) |
| MetaLR | Deleterious: MetaLR score $>$ 0.5; Tolerated: MetaLR score \leq 0.5 (Dong et al., 2015) |
| REVEL | Deleterious: REVEL score $>$ 0.5; Tolerated: REVEL score \leq 0.5 (Ioannidis et al., 2016) |